JOURNAL OF Materials CHEMISTRY

Effect of sizing on the surface properties of carbon fibres

Miguel A. Montes-Morán,* Amelia Martínez-Alonso and Juan M. D. Tascón

Instituto Nacional del Carbón, CSIC, Apartado 73, 33080 Oviedo, Spain

Received 22nd March 2002, Accepted 20th August 2002
First published as an Advance Article on the web 16th September 2002

Inverse gas chromatography (IGC) was used in this work to compare the surface properties of carbon fibres covered with two different amounts of an unknown sizing agent with those of fresh and industrially oxidised carbon fibres. Thermogravimetry and elemental analysis provided some clues about the nature of the sizing material. IGC results were analysed in terms of free energies, heats and entropies of adsorption, and surface free energies. Dynamic adsorption of *n*-alkanes showed that oxidation alone induces a high degree of disorder at the fibre surface, whereas sizing strongly reduces the surface energy of the fibres. Characterisation of the surface chemistry by adsorption of probe molecules with different acid–base character indicated that the oxidative treatment produces both acidic and basic groups, while sizing confers basic properties on the carbon fibre surface.

1. Introduction

Carbon fibres are being used extensively as a reinforcement in advanced composite materials owing to their outstanding mechanical properties. They are mainly employed in combination with polymer matrices as structural materials for aerospace applications and for the manufacture of prostheses and sports equipment. It is well established that the characteristics of the fibre/matrix interphase are a key factor in the performance of composites.[1–3] Therefore, carbon fibres usually receive a surface treatment in order to improve their adhesion to the matrix.[4,5] This treatment is aimed at enhancing the fibre–matrix interfacial adhesion, thus leading to composites with higher interlaminar shear strength. In terms of industrial production the most conventional surface treatment method used for carbon fibres is electrochemical oxidation.[4,5] This method offers the advantage of allowing continuous processing of fibres.

The manufacture of carbon fibres involves a latter stage in which fibres are coated with a thin layer of so-called sizing or finish. The main function of these sizings is to prevent the individual filaments of a fibre tow from contact damage between themselves or from eyelets or guides during weaving or prepregging. Additionally, many commercial sizings are formulated to be multifunctional, *i.e.*, to promote adhesion between the fibre and a given matrix. Sizings are thus critical in composite manufacturing and may or may not have positive effects on the final properties of the composite material. For example, coatings intended to avoid fibre damage may bond the filaments together and prevent uniform impregnation of the tows in the matrix.[5,6]

Unfortunately, the development of sizing agents is frequently an afterthought in composite materials technology. Indeed, the use of sizings as protective coatings is largely empirical, with relatively little documentation available. The choice is dictated by a number of considerations: good film-forming ability to coat the surface uniformly, compatibility with the matrix polymer, the level of filament protection required, environmental concerns, and cost.[6] It has to be mentioned that nowadays specific R&D departments in carbon fibre industries are considering proprietary sizing formulations that would not only protect the fibre but also enhance the composite's final properties. The optimum sizing content of the fibres is also a relevant issue in this area of research.[7]

In the present work, inverse gas chromatography (IGC) at infinite dilution has been selected to ascertain the effects brought about by different surface treatments (particularly sizing) on the surface of carbon fibres. The use of this technique involves a hierarchical characterisation of the material's surface properties. Elution of *n*-alkanes renders fundamental thermodynamic quantities related to dispersive interactions. These quantities can be related subsequently to changes in surface microstructure and/or texture. Finally, changes in surface chemistry are detected by eluting probes with polar character. From the information obtained from the elution of alkanes, the dispersive interactions can be subtracted from the overall interaction of the polar probe with the surface. In doing so, pure polar or specific interactions can be obtained, which are related directly to the chemistry of the material surface.[8–10]

2. Experimental

2.1. Materials

Fresh (untreated and unsized) high-strength, polyacrylonitrile-based carbon fibres (CF sample) were selected as the starting material, with typical values of 230 GPa and 3.3 GPa for the Young's modulus and tensile strength, respectively. A sample of CFO (*i.e.*, oxidised carbon fibres) consisting of CF carbon fibres oxidised (but unsized) following an unknown industrial method, was also characterised. According to the introduction it may be assumed that CFO was prepared following the conventional method of electrochemical oxidation.

Two sized samples, CFOA and CFOB, were studied subsequently. Both samples were prepared from CFO fibres. These were impregnated with a proprietary surface finish to make them compatible with epoxy resins. In principle, the difference between fibres CFOA and CFOB is the amount of sizing present on their surfaces, with CFOA fibres being less coated than CFOB ones, as stated in the manufacturer's information sheets.

2.2. Methods

Adsorption measurements were carried out by IGC at infinite dilution using a Hewlett-Packard 5890-II gas chromatograph equipped with a high sensitivity (10^{-12} mol) flame ionisation detector. Fibre yarns (1–3 g) were packed into approx. 40 cm long columns (2.40 mm in internal diameter) of passive nickel. Helium (99.9995% pure) was used as carrier gas. The gas flow rate F (15–35 ml min^{-1}) was measured at the column outlet (F_{flo}) by using a bubble flowmeter. Corrections were made for

the temperature difference between the column (T) and the flowmeter (T_{flo}), the water vapour pressure of the bubble (P_w), and the pressure drop (j is the correction factor, with P_{out} and P_{in} being the pressure at the outlet and inlet, respectively):[11]

$$F = jF_{flo}\frac{T}{T_{flo}}\left[\frac{(P_{out}-P_w)}{p_{out}}\right] \quad (1)$$

where,

$$j = \frac{3}{2}\left[\frac{(P_{in}-P_{out})^2-1}{(P_{in}-P_{out})^3-1}\right] \quad (2)$$

Adsorption experiments were carried out at 10 K intervals in the 303–353 ± 0.05 K temperature interval. For measurements obtained at the zero coverage limit, small amounts (0.1–1 μl) of vapours of *n*-alkanes (C_5–C_{12}) (>99% pure) measured with a 10 μl Hamilton syringe were eluted through the columns. Changes in the surface chemistry were evaluated by injecting several polar probes with different acid–base characteristics (nitromethane, carbon tetrachloride, acetone, diethyl ether and tetrahydrofuran, purity > 99%). At least five injections of each alkane were performed at each temperature. Methane was used to determine the dead volumes. No variation was detected in the retention volume of the probes when different flow rates were used. This indicates that the adsorption equilibrium was attained.[11]

Prior to the IGC experiments, the chromatographic columns were conditioned by heating at 383 K under a constant helium flow (~20 ml min^{-1}). Experiments showed that conditioning times of at least 50–60 h were necessary to achieve reproducible results, particularly with unsized samples CF and CFO. Moreover, it was found that the helium flow through the columns should not be interrupted anytime in the course of the experiments to avoid contamination by the laboratory atmosphere.

TG/DTG experiments were carried out in a Stanton-Redcroft STA-781 thermobalance provided with Plus-V data acquisition software (Rheometric Scientific). Samples (approx 20 mg) were placed in Pt crucibles 5 mm in diameter and 5 mm in depth. An constant flow of argon (99.999% pure by volume, 50 ml min^{-1}) at atmospheric pressure was used. Burning-off experiments were also performed, using a constant air (purity 99.999% by volume) flow of 50 ml min^{-1} at atmospheric pressure. Temperatures were measured with Pt/Rh thermocouples located at the bottom of the Pt crucibles and in contact with them.

3. Results

3.1. Thermal analysis

It was deemed necessary to determine the sizing content of fibres CFOA and CFOB. This content is defined as the percent of the total strand weight made up by the sizing, and it is usually determined by either dissolving the organic sizing or by burning off (also known as loss on ignition).[6] However, the use of an oxidising atmosphere at relatively high temperatures might render misleading results when determining the sizing content of carbon fibres, due to degradation of the raw carbon surfaces.

Alternatively, pyrolysis of the sized carbon samples was performed under argon at a linear heating rate of 10 K min^{-1} over the temperature range of 293–703 K , followed by an isothermal (703 K) stage during 30 min. Fig. 1 shows TG and DTG curves of samples CFOA and CFOB carried out under the conditions just described. Similar experiments were also performed with fibre CFO in order to validate the method for estimating the sizing content, *i.e.*, to verify that the weight loss experienced by CFOA and CFOB samples was only ascribable to sizing material. Results are also included in Fig. 1.

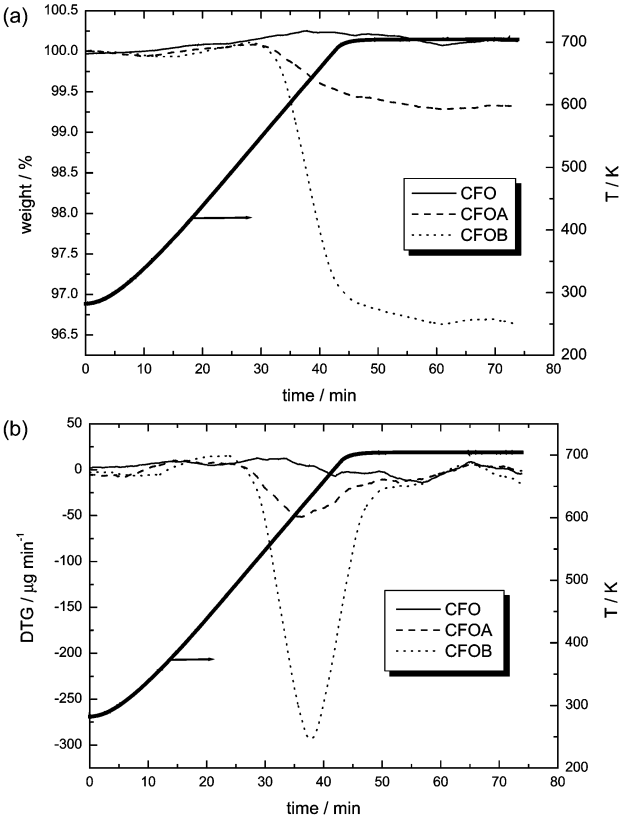

Fig. 1 (a) TG and (b) DTG curves for the pyrolysis of CFO, CFOA and CFOB samples. Also included is the temperature–time profile (thick line).

3.2. Adsorption of *n*-alkanes at zero coverage

The chromatographic peaks obtained for the *n*-alkanes were symmetrical for all samples under study, with no dependence of the peak maximum position on the amount of probe molecule injected. Under these conditions the adsorption can be considered to take place in the linear part of the isotherm (Henry's law), and the retention time of the different *n*-alkanes could be measured at the peak maximum.[11] The Henry's law constant, K_s, that characterises the adsorption equilibrium, is related directly to the retention volume V_N by:

$$V_N = K_s A \quad (3)$$

where A is the total surface area of the stationary phase. The previous equation is valid as long as the bulk adsorption of the probe in the stationary phase is negligible.[11,12] Thermodynamic functions of the adsorption process at infinite dilution can thus be calculated from K_s. The standard free energy of adsorption, ΔG^0_a was computed according to the following expression:

$$\Delta G^0_a = -RT\ln(K_s p_{s,g}/\pi_s) \quad (4)$$

where $p_{s,g}$ (pressure of the gas phase) and π_s (spreading pressure of the adsorbed gas) are constant parameters determined in the reference state.[13]

When zero coverage (or infinite dilution) conditions are fulfilled the standard differential heat of adsorption, q^0_d is numerically equal to the opposite of the enthalpy of the process. This value can be obtained from the variation of $-\Delta G^0_a$ with temperature. For an equilibrium process this variation is given by the Gibbs–Helmholtz equation,

$$\left[\frac{\partial(-\Delta G^0_a/T)}{\partial(1/T)}\right]_p = \left[R\frac{\partial(\ln K_s)}{\partial(1/T)}\right]_p = q^0_d \quad (5)$$

Fig. 2 illustrates the linear dependence of $(-\Delta G^0_a/T)$ as a function of $(1/T)$ obtained for the adsorption of *n*-heptane on

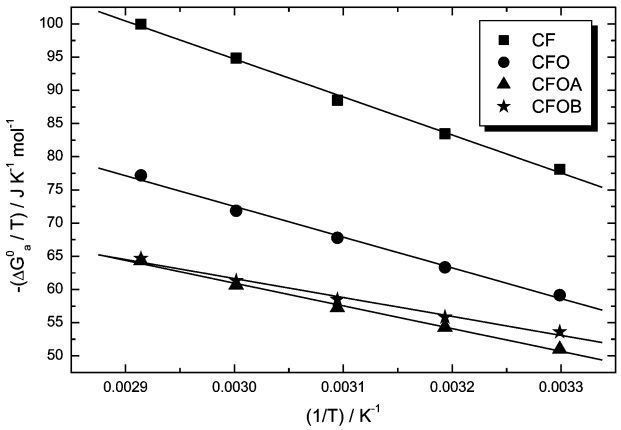

Fig. 2 Variation of $(-\Delta G^0_a/T)$ with $(1/T)$ for the adsorption of *n*-heptane on the carbon fibres under study.

the different carbon fibres under study. This behaviour, which is typical of the other hydrocarbons, implies that q^0_d is constant within the temperature range of characterisation. Values of the differential heats of adsorption at zero coverage for the different linear alkanes on the carbon fibre samples are collected in Table 1. The standard deviations in q^0_d values obtained in this way were never larger than 1%.

From the adsorption standard free energies and standard enthalpies, adsorption entropies were calculated easily according to:

$$\Delta S^0_a = -\frac{(q^0_d + \Delta G^0_a)}{T} \quad (6)$$

Table 2 gives the $-\Delta S^0_a$ values obtained for the carbon fibre samples. In agreement with the linearity in the $(-\Delta G^0_a/T)$ *vs.* $(1/T)$ plots (Fig. 2), the adsorption entropies were independent of temperature. Values collected in Table 2 are the average of

Table 1 Standard free energies and differential heats of adsorption of *n*-alkanes on the different samples (free energy at 343 K)

	q^0_d/kJ mol^{-1}				
n-Alkane	CF	CFO	CFOA	CFOB	$-\Delta H_{Liq}{}^a$/ kJ mol^{-1}
C_5	35.8	—	—	—	*25.5*
C_6	43.6	35.1	—	—	*30.3*
C_7	50.9	41.0	29.1	25.9	*35.0*
C_8	58.9	46.2	34.6	29.0	*39.8*
C_9	—	52.4	39.5	33.4	*44.6*
C_{10}	—	57.9	44.6	37.4	*49.4*
C_{11}	—	—	49.5	40.7	*54.2*
C_{12}	—	—	53.6	46.7	*58.9*

[a]Heats of liquefaction.

Table 2 Standard entropies of adsorption of *n*-alkanes on the different samples

	$-\Delta S^0_a$/J K^{-1}mol^{-1}				
n-Alkane	CFO	CFO	CFOA	CFOB	$-\Delta S^0_a{}^a$/ J K^{-1}mol^{-1}
C_5	62.1	—	—	—	*51.2*
C_6	72.5	60.4	—	—	*52.0*
C_7	82.1	69.0	39.9	28.7	*52.6*
C_8	93.6	75.4	49.7	31.1	*53.1*
C_9	—	84.9	57.4	37.7	*53.6*
C_{10}	—	91.7	66.1	42.6	*54.0*
C_{11}	—	—	74.0	45.6	*54.4*
C_{12}	—	—	79.5	56.9	*54.8*

[a]Standard entropy of adsorption (at 303 K) calculated according to de Boer's model [eqns. (9) and (10)].

data calculated at the different temperatures, deviations being smaller than 1%.

Values of the dispersive component of the surface free energy, γ^D_S were calculated using the formula proposed by Dorris and Gray:[14]

$$\frac{-\Delta G^{CH2}_a}{N_A a_{(CH2)}} = 2(\gamma_{(CH2)}\gamma^D_s)^{1/2} \quad (7)$$

where $-\Delta G^{CH2}{}_a$ is the difference in the free energy of adsorption of two *n*-alkanes with succeeding values of *n*, N_A is Avogadro's number, $a_{(CH2)}$ is the area of a methylene group (0.06 nm^2), and $\gamma_{(CH2)}$ is the surface tension of ideal liquid polyethylene. Fig. 3 illustrates the linear variations of $-\Delta G^0_a$ (at 343 K) with the number of carbon atoms in the series of *n*-alkanes used as probes. The slope of the regression lines corresponds to $-\Delta G^{CH2}{}_a$ for the different fibres, at a given temperature. Calculated γ^D_S values are plotted in Fig. 4 for the various carbon fibres within the range of temperatures studied. The error in the γ^D_S values is rather small (1–2%) due to the excellent data correlations obtained, similar to those shown in Fig. 3.

From the results shown in Fig. 4, the dependence of γ^D_S with temperature could be established. In all cases, it was found that linear expressions fit the experimental data reasonably well. Results corresponding to the linear regression of the data

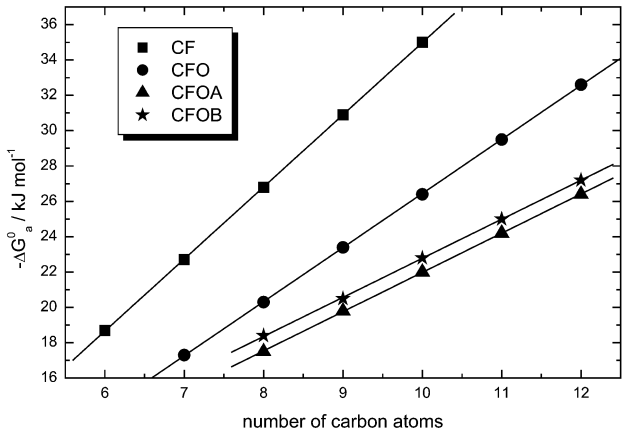

Fig. 3 Variation in the standard adsorption free energy $(-\Delta G^0_a)$ with the number of carbon atoms in the *n*-alkanes $(-\Delta G^0_a$ data at 343 K).

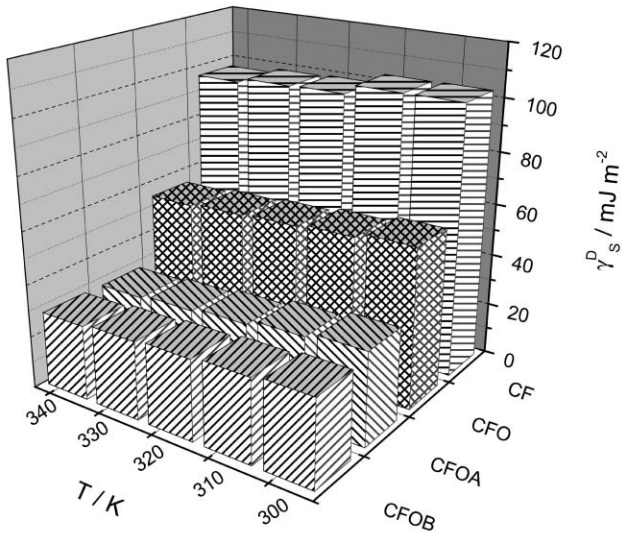

Fig. 4 Dispersive components of the surface free energy of carbon fibres at various temperatures.

Table 3 Dependence of γ^{D}_{S} (mJ m^{-2}) with temperature (K) for the carbon fibres under study

Fibre		r	$\gamma^{D}_{S}{}^{a}$/mJ m^{-2}
CF	$\gamma^{D}_{S} = 155.2 - 0.17T$	0.962	*105.4*
CFO	$\gamma^{D}_{S} = 102.8 - 0.14T$	0.992	*61.8*
CFOA	$\gamma^{D}_{S} = 89.6 - 0.18T$	0.995	*36.8*
CFOB	$\gamma^{D}_{S} = 66.0 - 0.11T$	0.999	*33.8*

[a]Values extrapolated to $T = 293.15$ K.

obtained for the different carbon samples are collected in Table 3. Values of γ^{D}_{S} at 293 K were subsequently calculated by extrapolation, and they are also included in Table 3.

3.3. Adsorption of polar probes at zero coverage

Whereas the adsorption of *n*-alkanes takes place through dispersive interactions thus rendering information related to fibre microstructure, polar probes are needed to determine the acid–base character of the fibre surfaces. The ability of these polar molecules to donate or accept electrons has been parametrised by means of the so-called donor number (DN) and acceptor number (AN), respectively.[15] Table 4 contains the DN and AN parameters of the probes used in this work.[15,16]

Slight concentration-dependent effects were observed for the elution of polar probes through all chromatographic columns. As a result, elution peaks of some of the compounds tested were asymmetric. The origin of this asymmetry should be the so-called "slow kinetic processes",[11] rather than being associated with instrumental problems (dead volumes in the detector or injector, imperfect column packing, *etc.*). Slow kinetic processes are characteristic of energetically heterogeneous surfaces containing preferential sites from which desorption takes place at a slower rate. They correspond to non-equilibrium situations so that the gas flow rate will have a significant effect on them. Different flow rates were tested, but no totally satisfactory results were obtained. Moreover, it was observed that the degree of asymmetry decreased dramatically when working at extremely low probe concentrations, *i.e.*, at low signal-to-noise ratio levels. Retention times were therefore estimated from the first momentum of the chromatographic peaks obtained under such conditions.

Similar thermodynamic properties to those described for the elution of linear alkanes can be obtained for the polar probes injected. Fig. 5 shows the variation of $(-\Delta G^{0}_{a}/T)$ *vs.* $(1/T)$ for all the polar probes on CFO samples. Similar plots were obtained for the rest of the carbon fibres under study. Reasonably good data regressions could be drawn. Values of standard enthalpies of adsorption (or differential heats of adsorption, eqn. (5)) were then calculated from the slopes of the lines depicted in Fig. 5. Table 5 shows the heats of adsorption of the polar probes onto the carbon fibre samples. Standard errors are once more relatively small, within the range of 2–3% of values collected in Table 5.

Two main components can be considered to contribute to the standard enthalpy of adsorption of polar probes, namely the specific contribution ΔH^{SP}_{a} and the dispersive contribution ΔH^{D}_{a}.[17]

Table 4 Donor numbers (DN) and acceptor numbers (AN) of the polar probes used in this work

Probe	AN/kJ mol^{-1}	DN/kJ mol^{-1}
Nitromethane	18.0	11.3
CCl_4	2.9	0
Acetone	10.5	71.1
Diethyl ether	5.9	80.3
THF	2.1	83.7

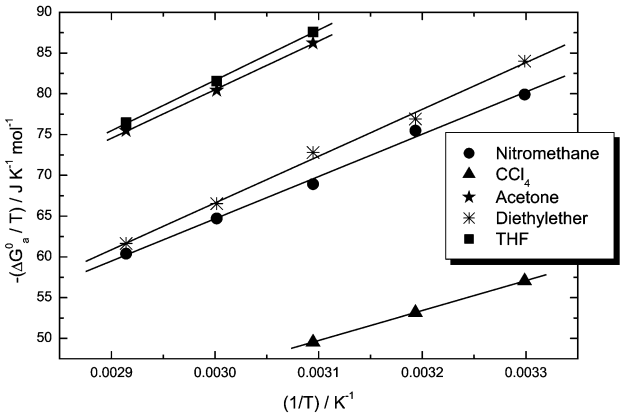

Fig. 5 Variation of $(-\Delta G^{0}_{a}/T)$ with $(1/T)$ for the adsorption of different polar probes on CFO sample.

Table 5 Differential heats of adsorption of several polar probes on carbon fibre surfaces

	q^{0}_{d}/kJ mol^{-1}				$-\Delta H_{Liq}{}^{a}$/ kJ mol^{-1}
	CF	CFO	CFOA	CFOB	
Nitromethane	36.2	47.6	34.1	34.0	*38.4*
CCl_4	41.4	36.7	24.0	23.8	*32.4*
Acetone	50.0	59.6	25.7	19.9	*31.3*
Diethyl ether	47.4	57.4	—	—	*27.4*
THF	51.6	61.8	25.0	21.9	*32.2*

[a]Heats of liquefaction.

$$\Delta H^{0}_{a} = \Delta H^{SP}_{a} + \Delta H^{D}_{a} \quad (8)$$

Several procedures have been developed to evaluate ΔH^{SP}_{a} from IGC measurements at zero surface coverage. The method proposed by Donnet *et al.*[18] seems to be more robust than the rest in accounting for the specific (acid–base) interaction of polar probes adsorbed on relatively high energetic surfaces.[19] This method takes into account the molecular polarisability of the different adsorbates. Specific interactions $(-\Delta G^{SP}_{a})$ are determined, at a given temperature, from the differences between $-\Delta G^{0}_{a}$ values of the polar probes and the reference line composed of data obtained from the elution of *n*-alkanes. An example of such a calculation for fibre CF is depicted in Fig. 6. Pertinent $-\Delta G^{SP}_{a}$ data for all fibres, at 303 K, are plotted in Fig. 7.

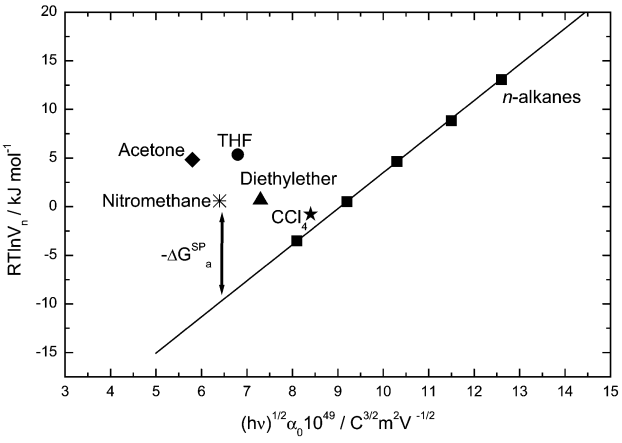

Fig. 6 Graphical description of the method followed to obtain the specific contribution of the adsorption free energy $-\Delta G^{SP}_{a}$ to the total value measured for the different polar probes. The solid line corresponds to the *n*-alkane trend line.

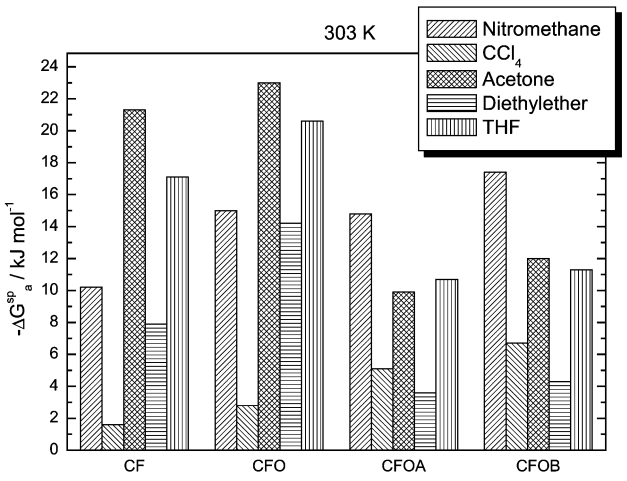

Fig. 7 $-\Delta G^{SP}{}_a$ values calculated for the adsorption of different polar probes on the carbon surfaces under study at 303 K.

$-\Delta H^{SP}{}_a$ can be now computed from the variation in $(-\Delta G^{SP}{}_a/T)$ *vs.* $(1/T)$, as stated in eqn. (5). This type of plot, corresponding to the adsorption data of polar probes on the CFOB sample, is shown in Fig. 8. The slopes of the lines depicted in Fig. 8 correspond to the value of $-\Delta H^{SP}{}_a$ for a particular probe adsorbed onto the carbon fibre surface. Results obtained for the different systems under study are collected in Table 6. Regressions of data similar to those appearing in Fig. 8 were occasionally rather poor. Individual standard errors are therefore included (in parentheses) in Table 6.

Herein values of $-\Delta G^{SP}{}_a$ and $-\Delta H^{SP}{}_a$ will be used as parameters to compare the acid–base character of the different carbon surfaces under study. These parameters can only account for qualitative changes in the surface chemistry of a given fibre. Further empirical approaches appearing in the literature would lead eventually to absolute parameters, similar to the AN and DN numbers mentioned earlier. In the present work, this procedure has been discarded on an operational basis. From the point of view of the calculations, the errors associated with $-\Delta H^{SP}{}_a$ values restrict, in some cases, their use in further parameter estimations. In other cases, when $-\Delta H^{SP}{}_a$ errors are acceptable, we experienced similar problems to those described quite recently when calculating absolute parameters to quantify the acid–base character of a solid surface: $(-\Delta H^{SP}{}_a/AN)$ *vs.* (DN/AN) plots of all polar probes tested lead to misleading results due to the substantial uncertainties of the final absolute parameters obtained.[19]

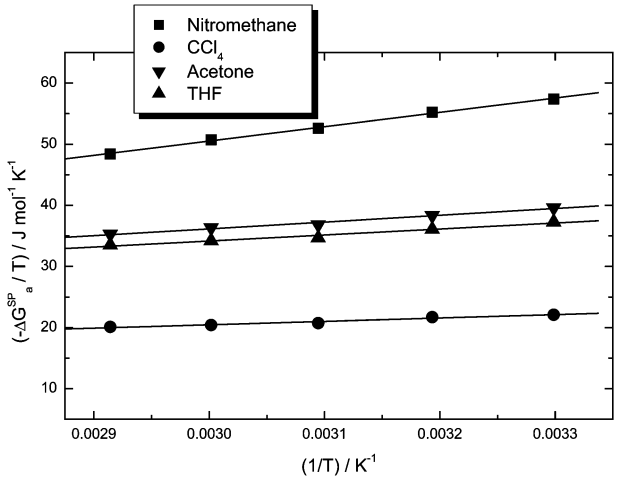

Fig. 8 Variation of $(-\Delta G^{SP}{}_a/T)$ with $(1/T)$ for the adsorption of different polar probes on the CFOB sample.

Table 6 Specific (acid–base) contributions to the standard enthalpy of adsorption of several polar probes on the carbon fibre surfaces

	$-\Delta H^{SP}{}_a$/kJ mol^{-1}			
	CF	CFO	CFOA	CFOB
Nitromethane	8.6 *(2.4)*	25.7 *(3.9)*	21.5 *(1.3)*	23.5 *(0.6)*
CCl_4	2.4 *(1.2)*	5.8 *(1.8)*	2.7 *(0.4)*	5.5 *(0.6)*
Acetone	26.2 *(3.8)*	40.0 *(0.7)*	7.0 *(4.2)*	11.1 *(0.8)*
Diethyl ether	15.0 *(2.8)*	31.1 *(2.0)*	—	—
THF	21.7 *(3.2)*	37.0 *(0.7)*	11.4 (1.0)	9.8 *(1.0)*

4. Discussion

Thermogravimetric analysis (Fig. 1) provided us with useful information regarding not only the amount of sizing present on fibres CFOA and CFOB but also about its prime constituents. The TG curves shown in Fig. 1a of the sized samples exhibit a single weight loss step starting at approx. 480 K. The unsized CFO fibre does not show any loss in weight within the temperature range explored. The small weight gain of the CFO TG curve is ascribed to experimental error. It is thus confirmed that the loss in weight of the CFOA and CFOB samples, approx. 0.7% and 3% in weight, respectively, can be assigned to their sizing content. The TG curves of CFOA and CFOB are, on the other hand, an indication that the type of coating present on both fibres is similar, which is confirmed when observing the DTG curves in Fig. 1b. The minima of the CFOA and CFOB DTG curves are almost coincident (~ 640 K), the differences being attributable to the lower resolution of the CFOA TG curve. The TG curves of the sized fibres (Fig. 1a) are very similar to that of the diglycidyl ether of bisphenol A (DGEBA),[20] a paradigmatic compound used in the epoxy resin industry.

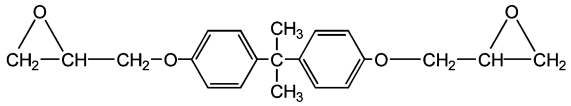

However, the DTG curves for the same fibres (Fig. 1b) revealed a slight difference to that of DGEBA: the minima of the DTG profiles is shifted towards a higher temperature (~ 640 K) than that observed for pure DGEBA (~573 K).[20] Such a shift is normally observed after curing the epoxy resin, *i.e.*, in a two component (resin–hardener) mixture.[21] The presence of an amine curing agent would also explain the results of the elemental analyses, based on the analysis of dry samples, performed on the carbon fibres under study (Table 7). As can be seen, there exists a significant increment in both oxygen content, ascribable to epoxy groups, and nitrogen content, presumably due to the presence of amine moieties, after fibre coating. The relatively high nitrogen content of non-coated fibres CF and CFO is attributable to the fibre precursor (polyacrylonitrile, PAN). Nevertheless, assuming that the sizing is formed mainly of DGEBA (density, 1.15 g cm^{-3}),[20] and that the carbon filaments (density,

Table 7 Elemental analyses (wt%) of sized and unsized carbon fibres (based on dry analysis)

Fibre	C	H	N	S	O
CF	94.06	-[a]	3.78	—	0.22
CFO	94.28	—	3.38	—	0.28
CFOA	93.09	—	4.06	—	0.43
CFOB	93.64	0.29	4.24	—	1.17

[a]Not detected (quantities below 0.05 wt%).

1.8 g cm^{-3}; diameter, 7.8 μm)[22] are homogeneously coated, it is estimated that the sizing layer thickness amounts to approx. 20 nm and 100 nm for CFOA and CFOB fibres, respectively.

As mentioned in the Results section, determination of sizing content on carbon fibres by means of their weight loss on ignition is not expected to be appropriate method. Fig. 9a shows preliminary burning-off experiments carried out on samples CFO and CFOB in air. The TG curve corresponding to the CFO fibres exhibits a progressive weight loss starting at 670 K, which indicates the oxidation of the bare fibre leading to a loss of carbon. Thus it seems apparent that the TG curve of CFOB under air comprises two different phenomena, *i.e.*, oxidation of sizing and burn-off of the bare carbon fibre. Subtraction of the CFOB from the CFO TG curves in air (dotted line, Fig. 9a) could still constitute an estimation of the CFOB sizing content if it is assumed that all sizing is removed prior to bare fibre oxidation. In other words, if the previous phenomena are consecutive, the percentage of sizing would be the weight loss detected at about 670 K, *i.e.*, approx. 3–3.5%, which compares well with results obtained in argon for CFOB (Fig. 1a). Fig. 9b depicts such a comparison, with the solid line being the TG curve of the CFOB sample in Ar and the dotted line being the curve obtained by subtraction of the CFOB curve from the CFO TG curve in air (*i.e.*, the dotted line of Fig. 9a). There exist significant differences between both curves in Fig. 9b despite the fact that their shapes are essentially the same. As expected, the starting point of weight loss in air is shifted to lower temperatures with respect to that of the pyrolysis experiment, due to the higher reactivity of the material in an oxygen atmosphere. However, the main difference between the curves of Fig. 9b is that the dotted line [$(TG_{CFOB} - TG_{CFO}) + 100$, in air] does not reach a plateau once the sizing is assumed to have been removed, as occurs in the Ar experiments. Instead, a persistent decrease in weight is observed. This would indicate that there exists an increment in the rate of oxidation of the bare carbon fibre once the coating is burnt-off from sample CFOB. Such a circumstance might be assisted by an increment in the temperature of the carbon fibre surface due to the exothermicity of the sizing combustion process.

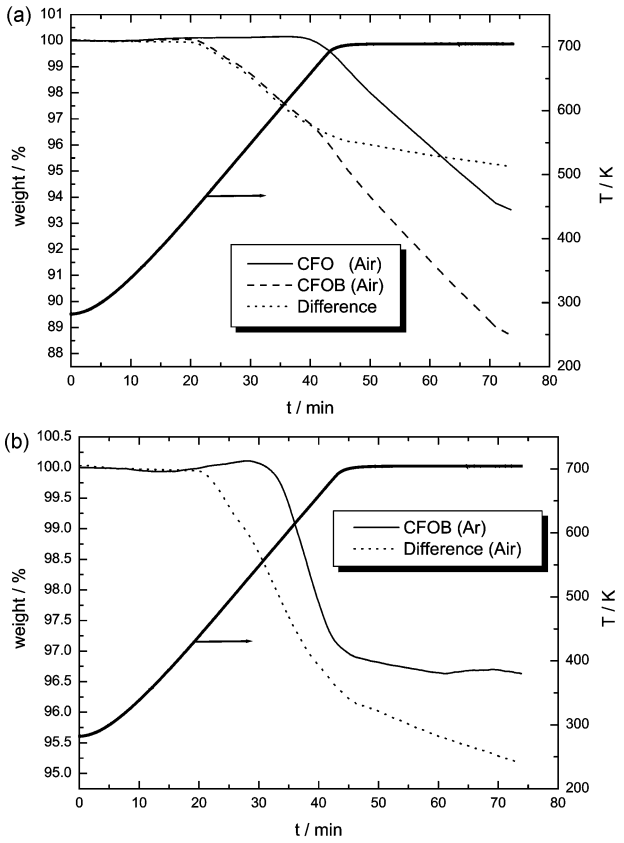

Fig. 9 (a) TG curves for CFO and CFOB samples obtained in air; the dotted line corresponds to the subtraction of CFOB and CFO TG curves, expressed in % (see text). (b) Comparison between the TG curves of CFOB in Ar (Fig. 1a) and the dotted line defined in Fig. 9a. Also included is the temperature–time profile (thick line).

IGC has demonstrated its usefulness for the surface characterisation of a wide range of materials.[8] Regarding the adsorption of linear alkanes, we have recently used this technique to ascertain the degree of surface heterogeneity (both energetic and nanostructural) brought about by different oxidative treatments on CF carbon fibres.[23] A detailed discussion of the effect of the commercial treatment (sample CFO) was then presented, and it allowed us to conclude that the structures accessible to *n*-alkane molecules in the industrially oxidized sample (CFO) seem to be highly disordered thus leading to a weaker interaction with the adsorbate.[23]

With a view to identifying the effect of sizing on the elution behaviour of the *n*-alkanes, results shown in the present work indicate that there exist qualitative differences in the thermodynamic parameters obtained for the unsized varieties, CF and CFO, and the sized carbon fibres under consideration. Fibre sizing leads to a systematic decrease in the probe–surface interaction energy, with CFOB sample values of q^0_d (Table 1) being the lowest of all the alkanes tested. Also shown in this table are the heats of liquefaction ($-\Delta H_{Liq}$) of the *n*-alkanes used at 323 K. The differential heats of adsorption of the *n*-alkanes on the CF and CFO fibre surfaces are larger than the heats of liquefaction, whereas lower values are obtained for the CFOA and CFOB fibres. The former behaviour (*i.e.*, $q^0_d > -\Delta H_{Liq}$) is typical of adsorption processes where adsorbate–adsorbent interactions are stronger than adsorbate–adsorbate interactions.[24] Furthermore, information on the CF fibre surface provided by zero-coverage IGC of non-polar probes is related mainly to graphitic structures, as discussed elsewhere.[23]

On the other hand, the behaviour of the sized fibres, with $q^0_d < -\Delta H_{Liq}$, might be considered anomalous, however, it has been reported several times. Chappell and Williams, for example, found the same behaviour in all the aramid fibres with surface finishes that they characterised,[25] independently of the particular finish composition. They also concluded that the complete isotherm of adsorption of *n*-alkanes on sized fibres would be Type III type according to the BDDT classification. This type of adsorption is representative of weak dispersive adsorbate–adsorbent interactions.[24]

A very similar conclusion can be reached from the analysis of the standard entropies of adsorption (Table 2). A progressive reduction in $-\Delta S^0_a$ absolute values is observed as the amount of fibre sizing increases, *i.e.*, when fibres CFO, CFOA and CFOB are compared. Also included in Table 2 are the adsorption entropy values predicted by an ideal adsorption model where the adsorbate is assumed to behave as a bidimensional gas.[12,13] According to this, the variation in the standard entropy of adsorption will coincide with the entropy decrease predicted by the loss of one translational degree of freedom, *i.e.* the difference between the translational entropies of a tridimensional ($_3S_t$) and a bidimensional gas ($_2S_t$), as given, respectively, by the statistical thermodynamic equations (9) and (10),

$$_3S_t = R \ln (M^{3/2}T^{5/2}) - 9.62 \quad (9)$$

$$_2S_t = R \ln (MTA_s) + 275.32 \quad (10)$$

where M is the molecular weight and A_s is the area occupied by one molecule in the standard adsorption state ($4.08T \times 10^{-16}$ cm^2). As Table 2 shows, the experimental adsorption entropies for the CF and CFO samples are larger (in absolute value) than those predicted by theory. This means that the

adsorbed hydrocarbons are more ordered than is predicted by the bidimensional gas model, involving the additional loss of some vibrational and/or rotational degrees of freedom. In other words, adsorbed molecules have a mobility lower than those with free movement over the surface. In contrast, entropies of adsorption for the CFOB sample are lower than theoretically predicted (Table 2). In this case, alkane molecules on the fibre surface are more disordered than is predicted by the bidimensional gas model. The positive contribution to the entropy can be assigned to mixing between the adsorbed molecules and surface contaminants. It must be stressed here that the possibility of probe absorption (*i.e.*, diffusion into the bulk material) is negligible due to the operational conditions of IGC at zero coverage. As regards the CFOA sample, the low sizing content surface exhibits intermediate behaviour. That is, absolute $-\Delta S^0_a$ values of medium length alkanes such as *n*-heptane and *n*-octane are much lower than is predicted by de Boer's model, whereas $-\Delta S^0_a$ values of *n*-nonane and succeeding alkanes are higher than the theoretical estimations.

These differences in the adsorption of *n*-alkanes on the carbon fibres under study are summarised in Fig. 10, where q^0_d *vs.* $-\Delta S^0_a$ data of Tables 1 and 2 are plotted against each other. Such a plot is associated with the compensation effect,[26] and it is used currently to highlight the differences in adsorbate–adsorbent interactions.[24,26] When a straight line fits the data of a compensation effect plot well it indicates the non-specific nature of the adsorbate–adsorbent interactions. In the case of Fig. 10, three straight lines are depicted, one corresponding to the data regression of CF and CFO, and two more fitting the CFOA and CFOB points. Although the line of CFOB is clearly shifted with respect to that of the unsized fibres, the slope of both lines is virtually the same and different from that of the CFOA fibre. Since the adsorbate type is the same (*n*-alkanes) for both sets of data, the difference in slopes cannot be assigned to specific interactions between the probes and the surfaces. Instead, it seems more likely that this effect is attributed to the existence of two different non-specific surfaces, one of the CFOB type of fibre and the other represented by the unsized fibres CF and CFO, with the CFOA fibre exhibiting intermediate characteristics.

Analysis of the dispersive component of the surface tension of carbon fibres γ^D_S (which, for comparative purposes, can be considered as the difference between the free energies of alkanes differing in one methylene group) leads to similar conclusions (Fig. 4) to those pointed out when discussing the differential heats of adsorption (Table 1). The presence of sizing lowers the dispersive component of the surface tension of the carbon fibres. This result agrees with previous research work performed with sized carbon[19,27] and aramid[19,25,28] fibres.

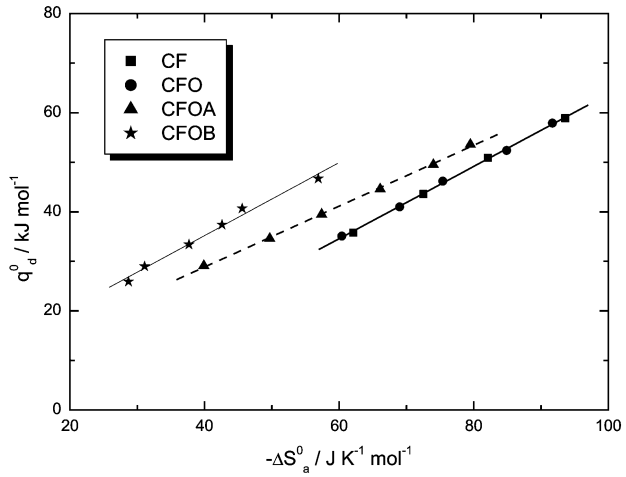

Fig. 10 The compensation effect.

It also reflects the fact that the surface characterisation of CFOA and CFOB fibres gives information relating to the sizing substance, which has a considerable lower surface tension than that of the pseudo-graphitic carbon surfaces of the unsized versions. Moreover, IGC is sensitive to the coating layer thickness; the thicker the layer (sample CFOB) the greater the decrease in γ^D_S.

One final remark related to the adsorption of linear alkanes on the series of fibres under study concerns the systematic differences between values of the thermodynamic quantities observed for fibres CFOA and CFOB. Indeed, sample CFOA has shown a behaviour intermediate between fibres CFO and CFOB in the adsorption of *n*-alkanes. Given that the coating substance is assumed to be the same on both sized fibres (see Experimental section), such a systematic difference should not be expected. Two possible reasons would explain this intermediate behaviour of fibre CFOA. The first assumes a perfect distribution of the sizing around the individual filaments. Due to the low thickness of the sizing layer in the case of fibre CFOA (20 nm as stated above), diffusion of the probe molecules into the coating would put them in contact with the carbon surfaces, thus provoking an increase in the adsorbate–adsorbent interaction. This possibility seems however to be unrealistic since bulk adsorption is minimised under the operational conditions of IGC measurements at zero surface coverage.[11] An alternative, more plausible, possibility presumes an uneven distribution of the coating around the filaments, due to the low sizing content of fibre CFOA. Evidence of such a situation, with sizing not entirely covering the surface of the fibre, has been reported previously.[29] Accessibility of the probe molecules to the unsized "islands" would bring about an increment in the average degree of fibre–alkane interaction.

Apart from changes in the adsorption of the *n*-alkanes, electrooxidative treatment (CFO) or the presence of sizings (CFOA, CFOB) on the fresh carbon fibres (CF) should also affect the chemical attributes of their surface. As the results in Table 5 reveal, analogous to the case of the linear hydrocarbons, $q^0_d < -\Delta H_{Liq}$ for all polar probes eluted through the CFOA and CFOB columns, whereas the opposite is observed for the CF and CFO fibres. Similar arguments thus prevail, *i.e.*, weak adsorbate–adsorbent interactions are characteristic of the adsorption process of polar molecules onto sized surfaces.

Direct comparison of differential heats of adsorption values in Table 5 can be misleading both between different polar probes within a given sample, or between the same probe and different solid surfaces. The reason following the first is obvious since the molecular dimensions and polar character of the adsorbates are different. As for the second situation, a correct comparison could only be made if the magnitude of the dispersive interactions exerted by the solid surfaces is similar, which is not the case for the samples under study. These drawbacks are circumvented when specific components of thermodynamic quantities $-\Delta G^{SP}_a$ and $-\Delta H^{SP}_a$ are compared (Fig. 7 and Table 6, respectively). As mentioned before, errors in $-\Delta G^{SP}_a$ data are much lower than those of $-\Delta H^{SP}_a$. Since the trends followed by both quantities are broadly the same, it is preferable to relate the changes in the polarity of the carbon fibres to the $-\Delta G^{SP}_a$ values (Fig. 7). In doing so, several features appear to be relevant.

Starting with the effect of the oxidative treatment, it can be seen (Fig. 7) that there is a noticeable increase in $-\Delta G^{SP}_a$ values corresponding to the adsorption of acidic (nitromethane) and basic (diethyl ether and THF) probes onto CFO fibres, compared with those obtained for the CF sample. Additionally, the specific contribution to the overall free energy of adsorption of the apolar (carbon tetrachloride) and amphoteric (acetone) molecules remains almost unaltered after surface treatment. On the other hand, the subsequent coating of the CFO fibre (CFOA and CFOB samples) brings about a

drastic reduction in $-\Delta G^{SP}_a$ values obtained for the basic and amphoteric probes. Conversely, the $-\Delta G^{SP}_a$ values for nitromethane adsorbed on sized fibres are similar (fibre CFOA) or even greater (fibre CFOB) than that for fibre CFO. A slight increment in the specific contribution to the overall free energy of adsorption of the apolar carbon tetrachloride is also observed after coating the CFO fibres.

The use of specific parameters such as $-\Delta G^{SP}_a$ or $-\Delta H^{SP}_a$ does not allow one to establish the overall acidic or basic character of the fibres under study, as was mentioned in the previous section (Results). However, qualitative changes in the acid–base character of different fibres can be ascertained by means of $-\Delta G^{SP}_a$ data. For example, it can be seen from Fig. 7 that the trends followed by the different probes on the unsized fibres CF and CFO are very similar, changes being only related to the absolute values of $-\Delta G^{SP}_a$. The higher values of $-\Delta G^{SP}_a$ observed after fibre oxidation are attributable to an increment of the strength and/or amount of both acidic and basic surface sites created after oxidative treatment. This observation agrees with previous results[5,30] which have reported a substantial increase in surface oxygen-containing species of different acid–base characteristics (carboxys, lactones, phenolic alcohols, ketones and/or pyrones) after electrochemical treatment of high strength carbon fibres.

Concerning the effect of sizing, it can be seen from Fig. 7 that the basic character of the carbon fibres increases after coating their surfaces. Indeed, the $-\Delta G^{SP}_a$ ratio of the basic (diethyl ether or THF) to the acidic probe (nitromethane) gives a clear indication of CFOA and CFOB surfaces being more basic than CFO ones. This result is consistent with the previous hypothesis of a two component resin–hardener sizing (Fig. 1b and Table 7). The presence of amino functionalities would considerably enhance the basicity of the carbon fibre surfaces, in agreement with results shown in Fig. 7.[31] Finally, CFOA and CFOB fibres also show the highest specific contribution to the free energy of adsorption of the apolar carbon tetrachloride when compared to the unsized of samples, which in turn exhibit very similar values of $-\Delta G^{SP}_{a(CCl4)}$. Such relatively high values of $-\Delta G^{SP}_{a(CCl4)}$ obtained for the sized fibres might be explained in terms of entropy contributions to the free energy of adsorption, since the multipole interactions expected in the adsorption of carbon tetrachloride should not amount to much more than pure dispersive interactions.

5. Conclusion

Changes in the surface properties of carbon fibres submitted to oxidative treatment and subsequent sizing have been investigated by means of IGC adsorption studies. On one hand, the structures accessible to *n*-alkane molecules in the industrially oxidized sample seem to be highly disordered thus leading to weaker interactions with the adsorbate. This type of treatment also brings about a considerable increase in the number and/or strength of both acidic and basic sites present on the original carbon surfaces. On the other hand, the use of sizings has been shown to reduce dramatically the surface energy of the fibres, as measured by the dynamic adsorption of *n*-alkanes. Moreover, the surface chemistry of the fibres is modified greatly as a consequence of surface coating. In particular, sized fibres exhibit a more basic character when compared to the unsized fibres. IGC is also sensitive to differences in the fibre sizing content, these being reflected in the adsorption behaviour of both alkanes and polar probes. Overall, IGC has been demonstrated to be a very suitable technique for characterising the changes in fibre surface properties following oxidation and sizing treatments.

Acknowledgements

Financial support from DGICYT (project PB98-0492) is gratefully acknowledged. One of the authors (M. A. M-M.) thanks FICYT (Spain) for a personal grant.

References

1 P. Ehrburger and J. B. Donnet, in *Strong Fibres*, ed. W. Watt and B.V. Perov, North-Holland, Amsterdam, 1985, p. 577.
2 J. B. Donnet and G. Guilpain, *Carbon*, 1989, **27**, 749–757.
3 L. H. Sharpe, in *The Interfacial Interactions in Polymeric Composites*, ed. G. Akovali, Kluwer, Dordrecht, 1993, p. 1.
4 E. Fitzer, in *Carbon Fibers, Filaments and Composites*, ed. J. L. Figueiredo, C. A. Bernardo, R. T. K. Baker and K. J. Hüttinger, Kluwer, Dordrecht, 1990, p. 3.
5 J. M. C. Peng, J.-B. Donnet, T. K. Wang and S. Rebouillat, in *Carbon Fibers*, ed. J.-B. Donnet, T. K. Wang, J. C. M. Peng and S. Rebouillat, Marcel Dekker, New York, 1998, p.161.
6 W. D. Bascom, in *Engineered Materials Handbook, Vol 1, Composites*, ASM International, Metals Park (OH), 1987, p. 122.
7 (*a*) P. J. de Lange and J. W. G. Mahy, *Fresenius J. Anal. Chem.*, 1995, **353**, 487–493; (*b*) J. H. Cramer, G. C. Tesoro and D. R. Uhlmann, *Ind. Eng. Chem. Prod. Res. Dev.*, 1982, **21**, 185–190.
8 *Inverse Gas Chromatography. Characterization of Polymers and Other Materials*, ed. D. R. Lloyd, T. C. Ward, H. P. Schreiber and C. C. Pizaña, ACS, Washington DC, (ACS Symp. Ser. No. 391), 1989.
9 M. M. Chehimi and E. Pigois-Landureau, *J. Mater. Chem.*, 1994, **4**, 741–745.
10 U. Panzer and H. P. Schreiber, *Macromolecules*, 1992, **25**, 3633–3637.
11 J. R. Conder and C. L. Young, *Physicochemical Measurements by Gas Chromatography*. Wiley, Chichester, 1979.
12 J. Vukov and D. G. Gray, *Langmuir*, 1988, **4**, 743–748.
13 J. H. De Boer, *The Dynamic Character of Adsorption*, Clarendon Press, Oxford, 1953.
14 G. M. Dorris and D. G. Gray, *J. Colloid Interface Sci.*, 1980, **77**, 353–362.
15 V. Gutmann, *The Donor-Acceptor Approach to Molecular Interactions*, Plenum Press, New York, 1979.
16 F. L. Riddle and F. M. Fowkes, *J. Am. Chem. Soc.*, 1990, **112**, 3259–3264.
17 (*a*) F. M Fowkes, *Ind. Eng. Chem.*, 1964, **56**, 40–52; (*b*) F. M. Fowkes and M. A. Mostafa, *Ind. Eng. Chem. Prod. Res. Dev.*, 1978, **17**, 3–7.
18 J. B. Donnet, S. J. Park and H. Balard, *Chromatographia*, 1991, **31**, 434–440.
19 A. Van Asten, N. van Veenendaal and S. Koster, *J. Chromatogr., A*, 2000, **888**, 175–196.
20 *Engineered Materials Handbook, Vol 1, Composites*, ASM International, Metals Park (OH), 1987, p. 399.
21 J.-Y. Lee, M.-J. Shim and S.-W. Kim, *J. Mater. Sci.*, 2001, **36**, 4405–4409.
22 Manufacturer's data sheet.
23 M. A. Montes-Morán, J. I. Paredes, A. Martínez-Alonso and J. M. D. Tascón, *J. Colloid Interface Sci.*, 2002, **247**, 290–302.
24 V. Kiselev and Y. I. Yashin, *Gas Adsorption Chromatography*, Plenum Press, New York, 1969.
25 P. J. C. Chappell and D. R. Williams, *J. Adhes. Sci. Technol*, 1990, **4**, 7–16.
26 (*a*) M. Domingo-García, I. Fernández-Morales, F. J. López-Garzón, C. Moreno-Castilla and M. J. Prados-Ramírez, *J. Colloid Interface Sci.*, 1990, **136**, 160–167; (*b*) F. Carrasco-Marín, M. Domingo-García, I. Fernández-Morales and F. J. López-Garzón, *Carbon*, 1991, **136**, 629–634.
27 (*a*) L. Lavielle and J. Schultz, *Langmuir*, 1991, **7**, 978–981; (*b*) J. Schultz, L. Lavielle and C. Martin, *J. Adhes.*, 1987, **23**, 45–60.
28 M. A. Montes-Morán, J. I. Paredes, A. Martínez-Alonso and J. M. D. Tascón, *Macromolecules*, 2002, **35**, 5085–5096.
29 N. J. Reis, A. M. Botelho do Rego and J. D. Lopes da Silva, *J. Mater. Sci.*, 1995, **30**, 118–126.
30 R. S. Farinato, S. S. Kaminski and J. L. Courter, *J. Adhes. Sci. Technol.*, 1990, **4**, 633–652.
31 U. Panzer, *Colloids Surfaces*, 1991, **57**, 369–374.